Marine Micropaleontology 70 (2009) 54–69

Contents lists available at ScienceDirect

Marine Micropaleontology

journal homepage: www.elsevier.com/locate/marmicro

Process length variation in cysts of a dinoflagellate, *Lingulodinium machaerophorum*, in surface sediments: Investigating its potential as salinity proxy

Kenneth N. Mertens [a,*], Sofia Ribeiro [b,bb], Ilham Bouimetarhan [c], Hulya Caner [d], Nathalie Combourieu Nebout [e], Barrie Dale [f], Anne De Vernal [g], Marianne Ellegaard [b], Mariana Filipova [h], Anna Godhe [cc], Evelyne Goubert [j], Kari Grøsfjeld [k], Ulrike Holzwarth [c], Ulrich Kotthoff [l], Suzanne A.G. Leroy [m], Laurent Londeix [n], Fabienne Marret [o], Kazumi Matsuoka [p], Peta J. Mudie [q], Lieven Naudts [r], José Luis Peña-Manjarrez [s], Agneta Persson [i], Speranta-Maria Popescu [t], Vera Pospelova [u], Francesca Sangiorgi [v], Marcel T.J. van der Meer [w], Annemiek Vink [x], Karin A.F. Zonneveld [y], Dries Vercauteren [z], Jelle Vlassenbroeck [aa], Stephen Louwye [a]

[a] *Research Unit Palaeontology, Ghent University, Krijgslaan 281 s8, 9000 Ghent, Belgium*
[b] *Department of Biology, Aquatic Biology Section, Faculty of Sciences, University of Copenhagen, Øster Farimagsgade 2D DK-1353 Copenhagen K, Denmark*
[c] *Centre for Marine Environmental Sciences (Marum), University of Bremen, P.O. Box 330440, D-28334, Germany*
[d] *Institute of Marine Sciences and Management, Istanbul University, Vefa 34470, Turkey*
[e] *LSCE/IPSL UMR CEA-CNRS-UVSQ, Domaine du CNRS, Avenue de la Terrasse Bat. 12, F-91198 Gif sur Yvette Cedex, France*
[f] *Department of Geosciences, University of Oslo, PB 1047 Blindern, N-0316 Oslo, Norway*
[g] *GEOTOP, Université du Québec à Montréal, P.O. Box 8888, Montréal, Québec, Canada H3C 3P8*
[h] *Museum of Natural History, 41 Maria Louisa Blvd., 9000 Varna, Bulgaria*
[i] *Department of Marine Ecology, Marine Botany, University of Gothenburg, PO Box 461, SE 405 30, Göteborg, Sweden*
[j] *Université Européenne de Bretagne, Université de Bretagne Sud, Lab-STICC, Campus Tohannic, 56 000 Vannes, France*
[k] *Geologikal Survey of Norway, N-7491 Trondheim, Norway*
[l] *Institute of Geosciences, University of Frankfurt, Altenhöferallee 1, D-60438 Frankfurt/M., Germany*
[m] *Institute for the Environment, Brunel University (West London), Uxbridge UB8 3PH, UK*
[n] *Université Bordeaux 1, UMR 5805 EPOC, avenue de Facultés, 33405 Talence cedex, France*
[o] *Department of Geography, University of Liverpool, Liverpool L69 7ZT, UK*
[p] *Institute for East China Sea Research (ECSER), 1-14, Bunkyo-machi, Nagasaki 852-8521, Japan*
[q] *Geological Survey Canada Atlantic, Dartmouth, Nova Scotia, Canada B2Y 4A2*
[r] *Renard Centre of Marine Geology (RCMG), Ghent University, Krijgslaan 281 s8, B-9000 Ghent, Belgium*
[s] *Centro de Estudios Tecnológicos del Mar No. 11. Km. 6.5 carretera Ensenada-Tijuana, Ensenada, Baja California, México*
[t] *Université Claude Bernard Lyon 1, Laboratoire PaléoEnvironnements et PaléobioSphère, UMR 5125 CNRD, 2 Rue Raphaël, Dubois, 69622 Villeurbanne Cedex, France*
[u] *School of Earth and Ocean Sciences, University of Victoria, Petch 168, P.O. Box 3055 STN CSC, Victoria, B.C., Canada V8W 3P6*
[v] *(Institute of Environmental Biology) Laboratory of Palaeobotany and Palynology Utrecht University, Utrecht, The Netherlands*
[w] *Marine Organic Biogeochemistry, NIOZ Royal Netherlands Institute for Sea Research, P.O. Box 59, 1790 AB Den Burg, Texel, The Netherlands*
[x] *Federal Institute for Geosciences and Natural Resources, Alfred-Bentz-Haus, Stilleweg 2, 30 655 Hannover, Germany*
[y] *Fachbereich 5-Geowissenschaften, University of Bremen, P.O. Box 330440, D-28334, Germany*
[z] *Laboratory of General Biochemistry and Physical Pharmacy, Ghent University, Harelbekestraat 72, 9000 Ghent, Belgium*
[aa] *UGCT, Ghent University, Proeftuinstraat 86, 9000 Ghent, Belgium*
[bb] *Departamento de Geologia Marinha, LNEG, Estrada da Portela, Zambujal 2721-866 Alfragide, Portugal Faculdade de Ciências, Universidade de Lisboa, Instituto de Oceanografia, Campo Grande 1749-016 Lisboa, Portugal*
[cc] *Department of Marine Ecology, University of Gothenburg, PO Box 461, SE 405 30, Göteborg, Sweden*

* Corresponding author. Tel.: +3292644613; fax: +3292644608.
E-mail address: Kenneth.Mertens@ugent.be (K.N. Mertens).

0377-8398/$ – see front matter
doi:10.1016/j.marmicro.2008.10.004

ARTICLE INFO

Article history:
Received 30 July 2008
Received in revised form 10 October 2008
Accepted 17 October 2008

Keywords:
Lingulodinium machaerophorum
Processes
Lingulodinium polyedrum
Biometry
Palaeosalinity
Dinoflagellate cysts

ABSTRACT

A biometrical analysis of the dinoflagellate cyst *Lingulodinium machaerophorum* [Deflandre, G., Cookson, I.C., 1955. Fossil microplankton from Australia late Mesozoic and Tertiary sediments. Australian journal of Marine and Freshwater Research 6: 242–313.] Wall, 1967 in 144 globally distributed surface sediment samples revealed that the average process length is related to summer salinity and temperature at a water depth of 30 m by the equation (salinity/temperature) = (0.078*average process length + 0.534) with R^2 = 0.69. This relationship can be used to reconstruct palaeosalinities, albeit with caution. The particular ecological window can be associated with known distributions of the corresponding motile stage *Lingulodinium polyedrum* (Stein) Dodge, 1989. Confocal laser microscopy showed that the average process length is positively related to the average distance between process bases (R^2 = 0.78), and negatively related to the number of processes (R^2 = 0.65). These results document the existence of two end members in cyst formation: one with many short, densely distributed processes and one with a few, long, widely spaced processes, which can be respectively related to low and high salinity/temperature ratios. Obstruction during formation of the cysts causes anomalous distributions of the processes. From a biological perspective, processes function to facilitate sinking of the cysts through clustering.

1. Introduction

Salinity contributes significantly to the density of seawater, and is an important parameter for tracking changes in ocean circulation and climate variation. Palaeosalinity reconstructions are of critical importance for better understanding of global climate change, since they can be linked to changes of the thermohaline circulation (Schmidt et al., 2004). Quantitative salinity reconstructions have been proposed on the basis of several approaches that use, for example, foraminiferal oxygen isotopes (e.g. Wang et al., 1995), $\delta^{18}O_{seawater}$ based on foraminiferal Mg/Ca ratios and $\delta^{18}O$ (e.g. Schmidt et al., 2004; Nürnberg and Groeneveld, 2006), alkenones (e.g. Rostek et al., 1993), the modern analogue technique applied to dinoflagellate cyst assemblages (e.g. de Vernal and Hillaire-Marcel, 2000) and δD in alkenones (e.g. Schouten et al., 2006; van der Meer et al., 2007, 2008). However, none of these approaches is unequivocal (e.g. alkenones; Bendle et al. 2005).

Some planktonic organisms are known to show morphological variability depending on salinity, e.g. variable noding in the ostracod *Cyprideis torosa*, van Harten (2000) and morphological variation in the coccoliths of *Emiliania huxleyi* (Bollman and Herrle, 2007). A similar dependence has been reported for *Lingulodinium machaerophorum* (Deflandre and Cookson, 1955) Wall, 1967, the cyst of the autotrophic dinoflagellate *Lingulodinium polyedrum* (Stein) Dodge, 1989 which forms extensive harmful algal blooms reported from California (Sweeney, 1975), Scotland (Lewis et al., 1985), British Columbia (Mudie et al., 2002), Morocco (Bennouna et al., 2002), West Iberia (Amorim et al., 2001) and other coastal areas. This species can be considered a model dinoflagellate since it is easily cultured and has been the subject of numerous investigations. An extensive review of these studies was given by Lewis and Hallett (1997).

Process length variation of *L. machaerophorum* was initially related to salinity variations in the Black Sea by Wall et al. (1973), and subsequently investigated in other regions (Turon, 1984; Dale, 1996; Matthiessen and Brenner, 1996; Nehring, 1994, 1997; Ellegaard, 2000; Mudie et al., 2001; Brenner, 2005; Sorrel et al., 2006; Marret et al., 2007). Kokinos and Anderson (1995) were the first to demonstrate the occurrence of different biometrical groups in culture experiments. Later culture experiments (Hallett, 1999) revealed a linear relationship between average process length and salinity, but also temperature.

The process length of *L. machaerophorum* as a salinity proxy represents a large potential for palaeoenvironmental studies, since this species occurs in a wide range of marine conditions (Marret and Zonneveld, 2003), and can be traced back to the Late Paleocene (Head et al., 1996). The aim of the present study was to evaluate whether the average process length shows a linear relationship to salinity and/or temperature, and to assess its usability for palaeosalinity reconstruction. To achieve this goal,

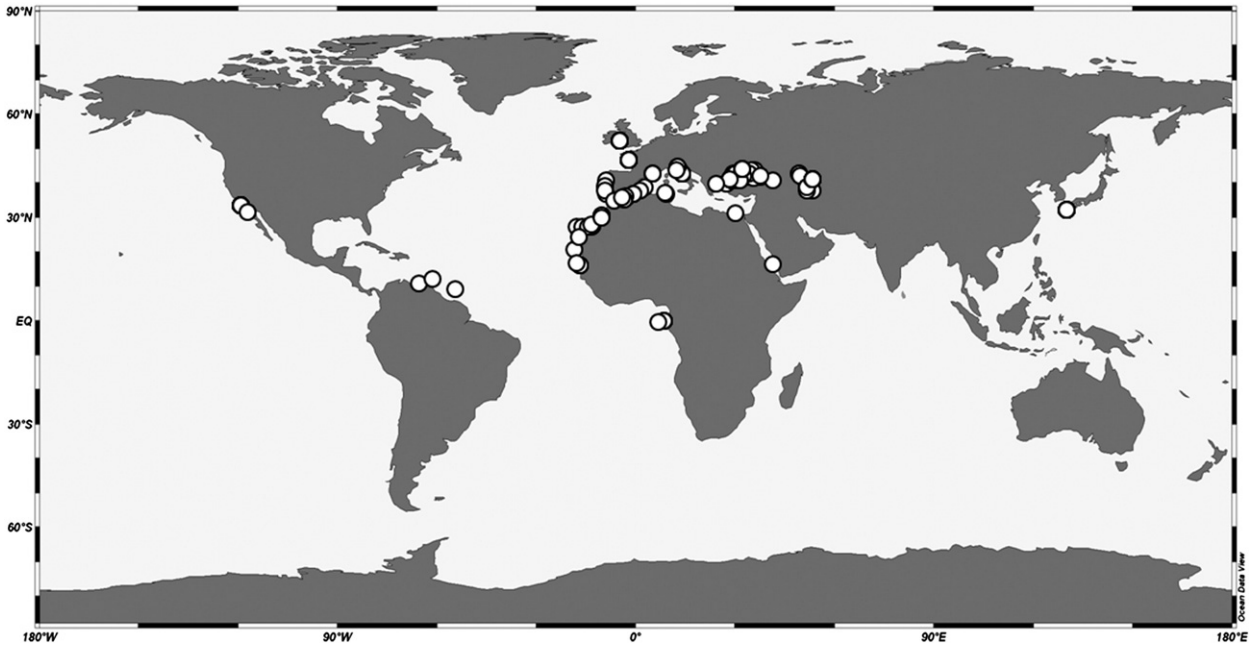

Fig. 1. Distribution of the 144 surface samples where *Lingulodinium machaerophorum* process lengths were studied.

Table 1
Average process length from LM measurements, standard deviation, body diameter and standard deviation, average summer temperature and salinity at 30 m water depth, ratio between both and density calculated from both

Region	# samples	Processes measured	Average process length (μm)	Stdev (μm)	Average body diameter (μm)	Stdev (μm)	Average summer $T_{30\ m}$	Average summer $S_{30\ m}$	$S_{30\ m}/T_{30\ m}$	Density (kg/m^3)	Preservation	Reference
Caspian Sea–Aral Sea	13	1320	5.6	3.4	48.1	6.1	15.72	12.72	0.81	1008.87	Bad to good	Marret et al. (2004), Sorrell et al. (2006), Leroy et al. (2006) and Leroy (unpublished data), Leroy et al. (2007)
Etang de Berre	2	300	7.5	2.5	44.9	4.5	19.91	26.10	1.31	1018.14	Average	Leroy (2001) and Robert et al. (2006)
Japan	5	735	8.0	1.9	45.3	5.7	24.54	33.72	1.37	1022.64	Good	Matsuoka (unpublished data)
Caribbean–West Equatorial Atlantic	6	306	13.0	4.4	44.1	6.4	26.19	36.08	1.38	1023.92	Average	Vink et al. (2000), Mertens et al. (2008) and Vink et al. (2001)
Scandinavian Fjords–Kattegat–Skagerrak	26	2271	13.2	4.2	47.9	6.4	16.55*	24.14*	1.46*	1017.43	Bad to good	Grøsfjeld and Harland (2001), Gundersen (1988), Ellegaard (2000), Christensen et al. (2004) and Persson et al. (2000)
East Equatorial Atlantic–Dakar Coast	7	903	13.2	3.4	46.6	6.2	22.88	35.52	1.55	1024.49	Bad to good	Marret (1994) and Bouimetarhan et al. (unpublished data).
Black Sea and Marmara Sea	35	5196	15.0	4.1	46.3	4.6	12.22	20.08	1.64	1015.14	Good	Verleye et al. (2008), Caner and Algan (2002), Caner (unpublished data), Cagatay et al. (2000), Naudts (unpublished data), Popescu et al. (unpublished), Mudie et al. (2007) and van der Meer et al. (2008)
Portugal–Brittanny	9	1350	16.8	3.6	45.3	5.5	16.53	35.22	2.13	1025.93	Good	Ribeiro et al. (unpublished data), Goubert (unpublished data)
NW Africa	12	1749	18.4	3.8	48.1	6.3	19.47	36.36	1.87	1026.07	Average to good	Holzwarth et al. (unpublished data); Kuhlmann et al. (2004), Richter et al.(2007)
Mediterranean–Red Sea	36	3507	19.6	4.4	45.6	6.1	18.39	37.57	2.04	1027.28	Average to good	Sangiorgi et al. (2005), Londeix (unpublished data), Combourieu-Nebout et al. (1999), Pirlet (unpublished data), Schoel (1974) and Kothoff et al. (2008)
Pacific	9	1224	21.2	4.3	47.7	6.1	14.39	33.45	2.32	1025.04	Good	Pospelova et al. (2008) and Peña-Manjarrez et al. (2005)
Celtic Sea	6	750	21.8	4.1	47.8	5.7	13.50	34.30	2.54	1025.88	Good	Marret and Scource (2002)

Results are sorted by short to long process length.
*For this region data from 0 m water depth is used.

L. machaerophorum cysts were studied from surface sediments collected in numerous coastal areas. Confocal laser microscopy was used for the reconstruction of the complete distribution of the processes on the cyst wall, which has important implications for cyst formation.

2. Material and methods

2.1. Sample preparation and light microscopy

A total of 144 surface sediment samples were studied for biometric measurements of *L. machaerophorum* cysts from the Kattegat–Skagerrak, Celtic Sea, Brittany, Portuguese coast, Etang de Berre (France), Mediterranean Sea, Marmara Sea, Black Sea, Caspian and Aral Seas, northwest African coast, Canary Islands, coast of Dakar, Gulf of Guinea, Caribbean Sea, Santa Monica Bay (California), Todos Santos Bay (Mexico) and Isahaya Bay (Japan) (Fig. 1). Most samples were core top samples from areas with relatively high sedimentation rates, and can be considered recent, i.e. representing a few centuries (see Supplementary data). Five samples have a maximum age of a few thousand years, but since process lengths are as long as processes of recent, nearby samples, these were also considered representative. In general, the studied cysts provide us a global view of the biometric variation of cysts formed during the last few

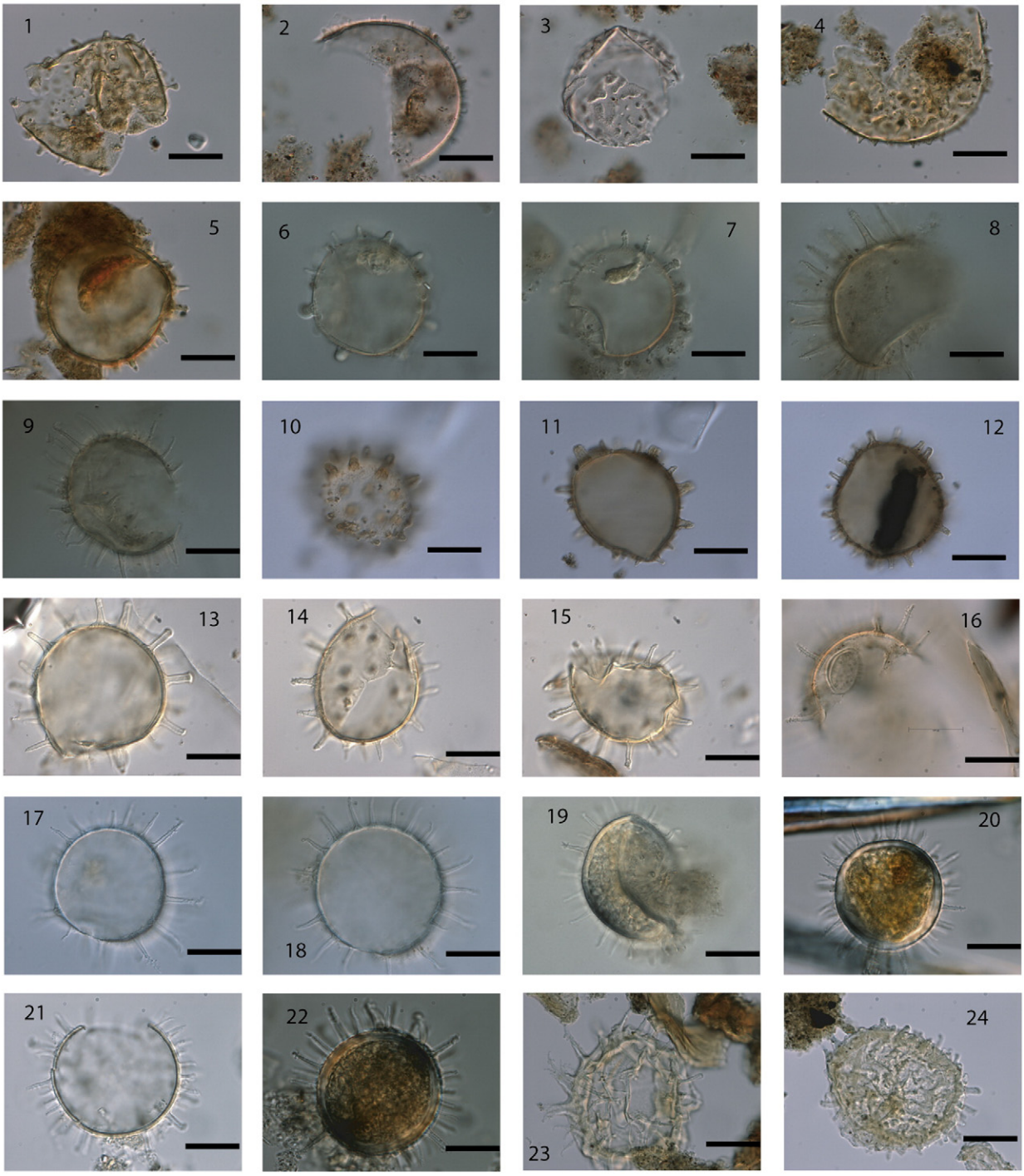

Plate I. *Lingulodinium machaerophorum* cysts from Caspian sea (1–5), Aral Sea (6–9), Etang de Berre (10–12). Baltic Sea (13–15) and Scandinavian Fjords (16–24). Specific sample names are 1–4. CPO4. 5.US02. 6–7. AR23. 8–9.AR17. 10–12. Etang de Berre (19). 13. NG6.14.NG.7.15.NG9.16. Limfjord. Note inclusion of *Nannobarbophora* acritarch. 17. Havstenfjorden 18–19. Guumar Fjord 20–21. G2.22.K2. 23–24. Risor Site. All scale bars are 20 µm.

centuries by *L. polyedrum*. It is assumed here that the environmental conditions steering the morphological changes within the cysts are similar to recent environmental conditions.

All the cysts were extracted from the sediments according to maceration methods that are described in the literature shown in Table 1. Most methods used standard maceration techniques involving hydrochloric acid and hydrofluoric acid, sieving and/or ultrasonication. Regardless of the method used, the cysts all appeared similar in terms of preservation (Plates I–IV).

All measurements were made using a Zeiss Axioskop 2 and an Olympus BH-2 light microscope, equipped with an AxioCam RC5 digital camera (Axiovision v. 4.6 software) and Color View II (Cell F Software Imaging System) respectively, and 100x oil immersion objectives. All measurements were performed by Kenneth Mertens, except for the samples from Portugal, which were measured by Sofia Ribeiro. Observer bias did not influence the measurements.

For each sample, the length of the three longest visible processes and the largest body diameter were measured of 50 cysts for each

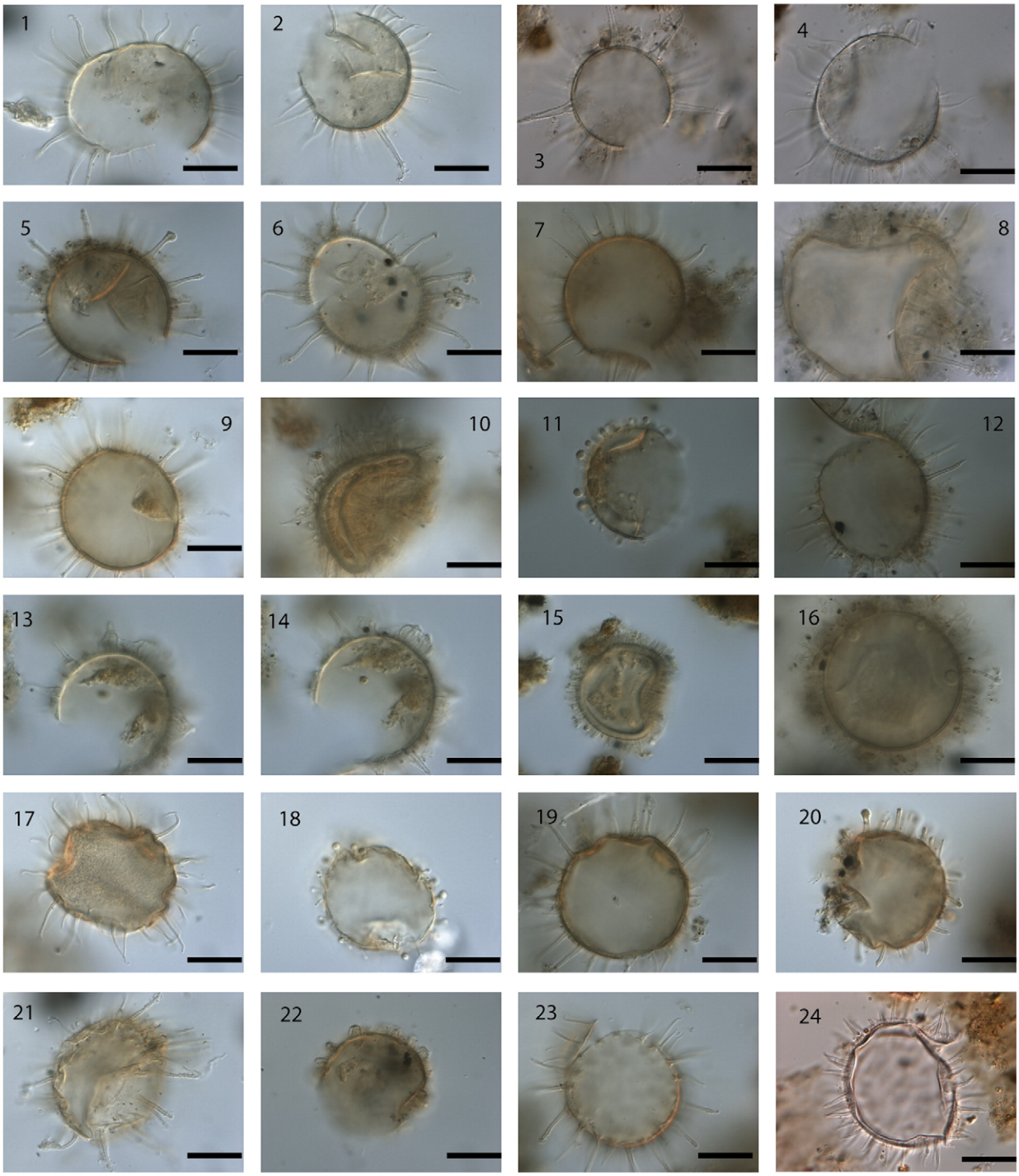

Plate II. *Lingulodinium machaerophorum* cyst from Marmara Sea (1–4) and Black Sea (5–24). Note the wide range of morphotypes occurring in these samples. Specific samples names are: (1–2) Dm 13 (3–4) Dm5 (5–6) Knorr 134.72. (7) Knorr 134.51. (8) GGC18 Swollen cyst due to use of acetolysis. (9–10) Knorr 134.35. (11–12) Knorr 134.2. (13–15) B2KS33 0-1. Note merged process in 13 and 14. (16) B2 KS 01 0-1. Note globules at basis of processes. (17–18) All 1464. (19) All 1443. (20–21) All 1438. (22) All 434. Note merged processes. (23) All145.1. (24) GeoB7625. Coloured with Safranin-O. All scale bars are 20 µm.

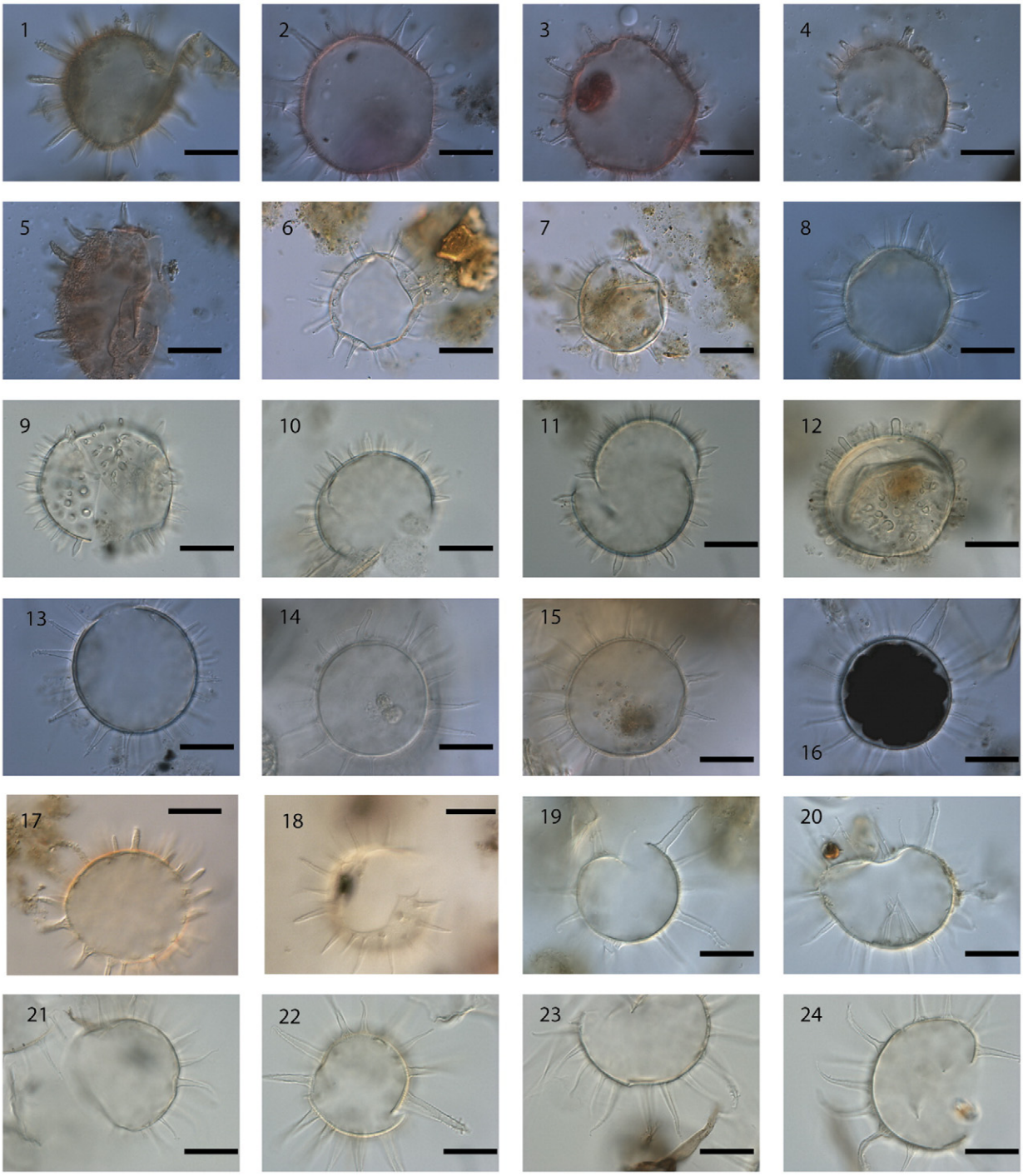

Plate III. *Lingulodinium machaerophorum* cyst from East Equatorial Atlantic (1–7), West Equatorial Atlantic (8), Japan (9–12), Brittanny (13–16), Portugal (17–18) and NW Africa (19–24). Specific sample names are: (1) 6437-1. (2–3) 6847-2. (4–5) 6875-1. (6–7) GeoB9503 Dakar. (8) M35003-4. (9–10) AB22. (11) AB40. (12) ISA2. (13) BV1. (14–15) BV3. (16) BV5. (17–18) Tejo. (19–20) GeoB4024-1 (21) GeoB5539-2. (22–24) GeoB5548. All scale bars are 20 µm.

sample. Measuring 50 cysts gave reproducible results: in sample GeoB7625-2 from the Black Sea, three process lengths per cyst for 50 cysts were measured, and was then repeated on 50 different cysts, showing no significant differences (x = 13.50 µm ± 2.99 µm and x = 13.21 µm ± 2.62 µm, t-test: p = 0.37). The length of each process was measured from the middle of the process base to the process tip. The absolute error in process measurement was 0.4 µm. Within each cyst, three processes could always be found within the focal plane of the light microscope, and for this reason this number seemed a reasonable choice. Three reasons can be advanced for choosing the longest processes. Firstly, the longest processes reflect unobstructed growth of the cyst (see below). Secondly, the longest processes allowed to document the largest variation, and this enhanced the accuracy of the proxy. Thirdly, since only a few processes were parallel to the focal plane of the microscope, it was imperative to make a consistent choice. Sometimes fewer than 50 cysts were measured, if more were not available. Fragments representing less than half of a cyst were not measured, nor were cysts with mostly broken processes.

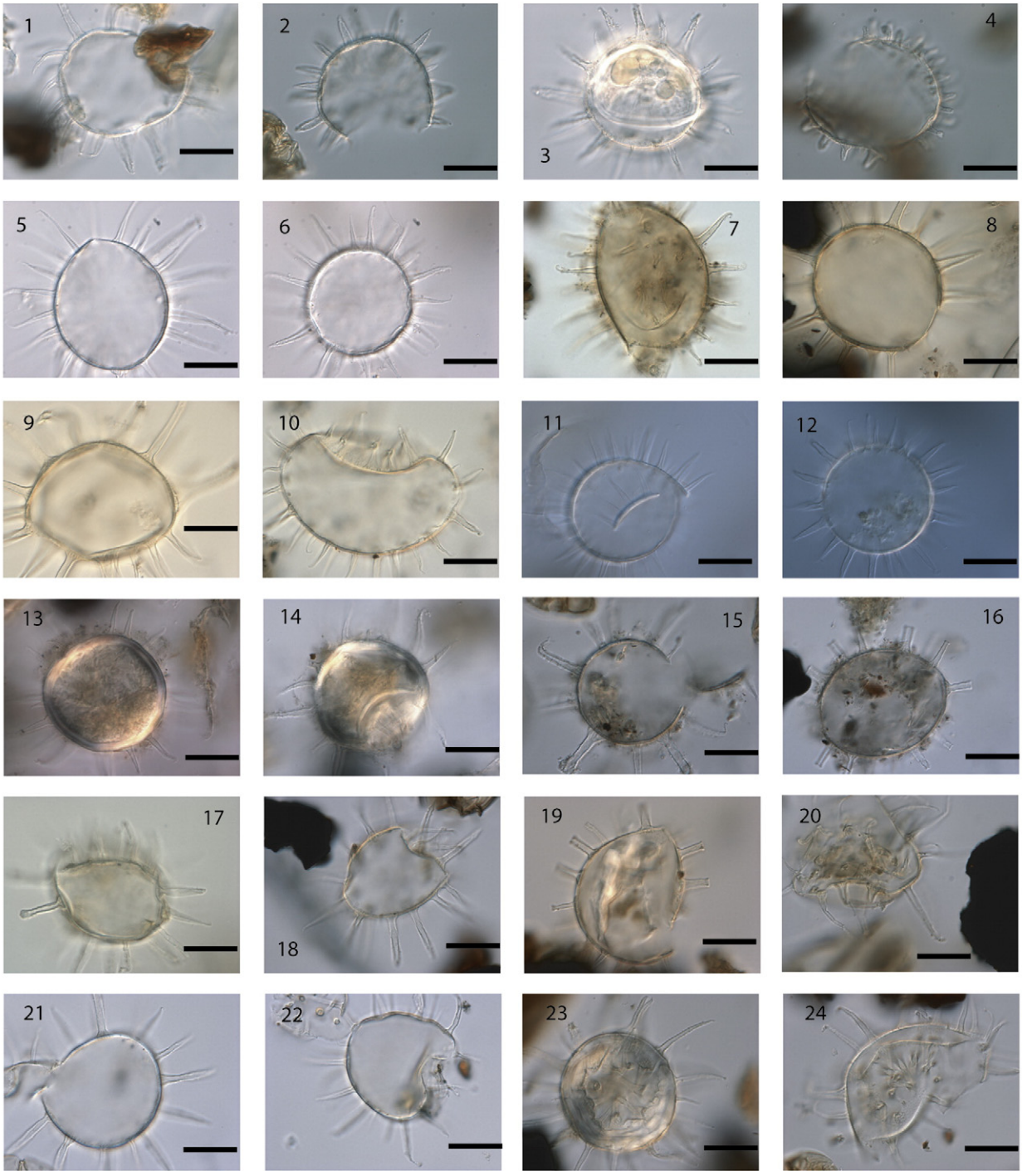

Plate IV. *Lingulodinium machaerophorum* cyst from Mediterranean (1–11), Red Sea (12) Celtic Sea (13–16) and Pacific Ocean (17–24). Note the widely distributed very long processes in Celtic Sea and Pacific Ocean samples. Specific samples are: (1) North Adriatic AN7l. (2–4) North Adriatic AN71. (5–6) Nile Delta. (7) 273.4. (8) 5153. (9) 516.6. (10) 521.3. (11–l2) Red Sea VA01-200P. (13–14) Station9 6.99. (15) Station 9 5.00 (16) Station 9 2.99 with truncated processes. (17) Todos Santos Bay (Mexico). (18–19) Santa Monica Bay,, UVic07-896 18 with truncated processes. (20) UVic07-897. (21–22) UVic07-898.22 with truncated processes. (23–24) UVic07-902. All scale bars are 20 µm.

2.2. Salinity and temperature data

The biometric measurements on cysts from the different study areas were compared to both seasonal and annual temperature and salinity at different depths — henceforth noted as $T_{0\ m}$, $T_{10\ m}$,... and $S_{0\ m}$, $S_{10\ m}$, ..., using the gridded 1/4° World Ocean Atlas 2001 (Stephens et al. 2002; Boyer et al., 2002) and the Ocean Data View software (Schlitzer, R., http://odv.awi.de, 2008). For the Scandinavian Fjords, in situ data were available from the Water Quality Association of the Bohus Coast (http://www.bvvf.com).

2.3. Confocal laser microscopy

Confocal microscopy was performed using a Nikon C1 confocal microscope with a laser wavelength of 488 nm and laser intensity of 10.3%. No colouring was necessary since the cysts were sufficiently autofluorescent. The Z-stack step size was 0.25 µm with a Pixel dwell time of 10.8 µs. The objective used was a 60×/1.40/0.13 Plan-Apochromat lens with oil immersion. After correcting the z-axis for differences in refractive index between the immersion oil and glycerine jelly (here a factor of 78% of correction was used), images

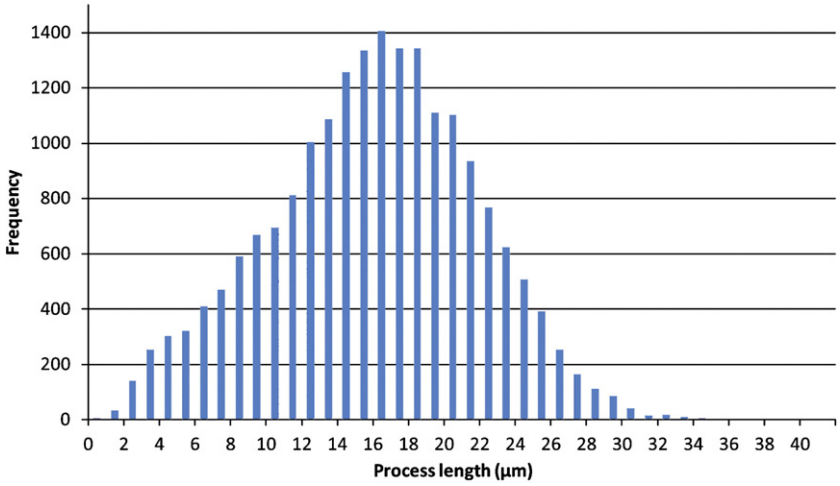

Fig. 2. Size-frequency spectrum of 19,611 process measurements.

were rendered to triangulated surfaces (.stl files) with Volume Graphics VGStudioMax© software. These were imported in Autodesk 3DsMax©, where XYZ coordinates of the base and top of the processes were recorded. From these coordinates Euclidean distances were calculated, enabling the calculation of the process length and the distances between the processes. Distances to the two closest processes of each process were calculated, and by averaging these numbers, the average distance between processes was calculated. A more detailed description of the methodology is given at http://www.paleo.ugent.be/Confocal.htm.

3. Results

3.1. Preservation issues

To establish the validity of the measurements, preservation needs to be taken into account. Two types of degradation were considered: mechanical and chemical. Three categories were used to describe the mechanical degradation of the cysts: bad (most cysts were fragmented or torn, and processes were broken), average (about half of the cysts were fragmented or torn, and few processes were broken, and good (few cysts were torn or fragmented, and were often still encysted) (see Table 1).

The differences in mechanical breakdown were, from our experience, largely caused by post-processing treatments such as sonication. Prolonged sonication, however, does not significantly change process length variation. The sample from Gullmar Fjord (average process length of 14.6 µm, standard deviation SD 4.0) was sonicated in an ultrasonic bath for two minutes and the results were not significantly different from samples that were not sonicated (average process length of 14.3 µm, SD 4.1) (*t*-test: $p=0.38$).

Chemical breakdown, on the other hand, could be caused by oxidation or acid treatment. *L. machaerophorum* is moderately sensitive to changes in oxygen availability (Zonneveld et al., 2001). Cysts from samples treated with acetolysis were clearly swollen (Plate II.8). Most interestingly, both processes and cyst body swell proportionately. These samples were not used for analysis. Similar results were noted after treatment with KOH. These maceration methods are not suitable for biometric studies. Cysts extracted using warm HF showed traces of degradation (see Plate I.23, I.24), but process length did not change.

3.2. Overall cyst biometrics for the multi-regional dataset

The 19,611 process length measurements resulted in a global average of 15.5 µm with a standard deviation of 5.8 µm, and a range from 0 to 41 µm (Fig. 2). Most cysts encountered were comparable to the forms described by Kokinos and Anderson (1995), and bald cysts were rare. The range found is clearly broader than the 2 to 21 µm range postulated by Reid (1974). The skewness of the distribution was −0.12, since there is some tailing at the left side of the size frequency curve (Fig. 2). The asymmetric distribution was due to the fact that standard deviation increased with average process length. This could be explained partly by the methodological approach – errors on the larger measurements were larger, since larger processes were more often curved or tilted – and by the more common occurrence of cysts with relatively shorter processes in samples that

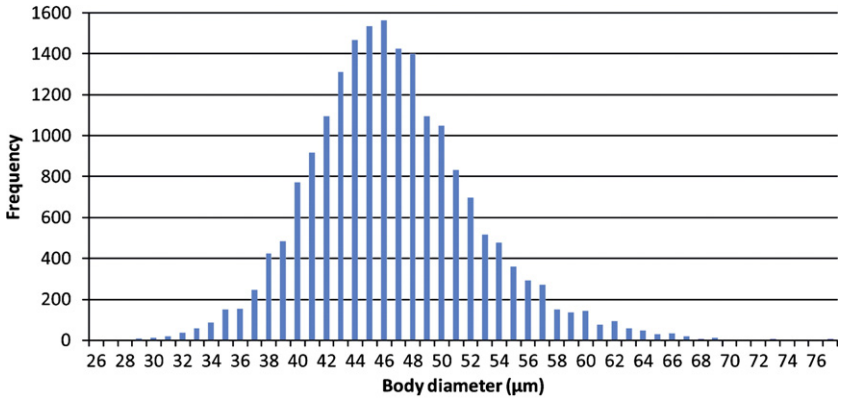

Fig. 3. Size-frequency spectrum of 6211 body diameter measurements.

mostly contain cysts with longer processes (also evident in regional size-spectra, Fig. 4).

The 6537 body diameter measurements resulted in an average body diameter of 46.6 µm with a standard deviation of 5.8 µm, over a range from 26 to 77 µm. This was again a broader range than the 31 to 54 µm given by Deflandre and Cookson (1955) and Wall and Dale (1968). This discrepancy could be explained partly by cysts sometimes being compressed or torn, yielding an anomalously long body diameter. This mechanical deformation of the cyst explains also a positive skewness of the size-frequency spectrum (Fig. 3).

The averaged data of *L. machaerophorum* cysts in every region is given in Table 1, sorted from low to high average process length. Individual size-frequency spectra are shown in Fig. 4 and the cysts are shown in Plate I–IV. All measurements are available as Supplementary data.

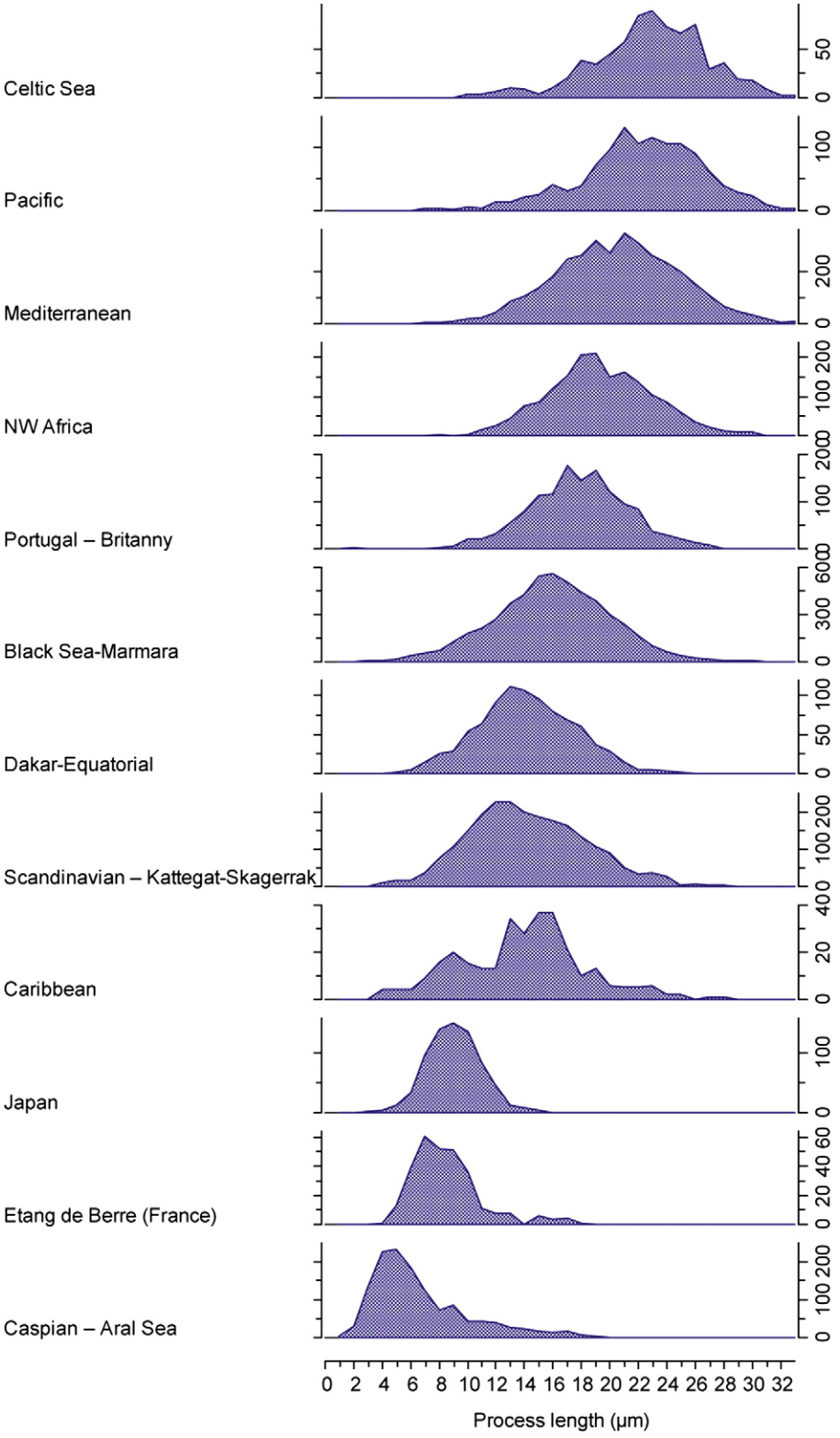

Fig. 4. Size-frequency spectra of regional process measurements, sorted from top (long average processes) to bottom (short average processes).

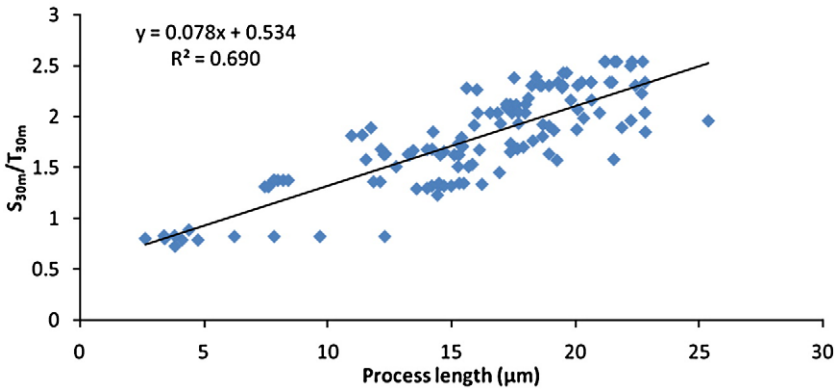

Fig. 5. Regression between average process length and summer $S_{30\ m}/T_{30\ m}$ for the 144 surface samples.

3.3. Comparison of process length with salinity and temperature

Data from the Scandinavian Fjords and the Kattegat–Skagerrak were excluded from all relations since they significantly increased the scatter on all regressions. The reason is given in the Discussion (Section 4.3).

The relation of the average process length of *L. machaerophorum* with only the salinity data, fitted best with the winter $S_{0\ m}$ (R^2=0.54). When compared to temperature data alone, the best relationship was with the winter $T_{50\ m}$ (R^2=0.06). A much stronger relationship could be found with salinity divided by temperature at a water depth of 30 m from July to September (summer). This relationship is expressed as ($S_{30\ m}/T_{30\ m}$)=(0.078*average process length+0.534), and has a R^2=0.69 (Fig. 5) and the standard error is 0.31 psu/°C. Since seawater density is dependent on salinity and temperature, it could be expected that density would have a similar relationship with process length. However, the regression with water density at 30 m water depth shows a stronger relation to process length (R^2=0.50) than with salinity alone (R^2=0.42 with summer $S_{30\ m}$), but not better than with $S_{30\ m}/T_{30\ m}$.

An overview of the results in the studied areas is given in Table 1. Next to average process length, salinity, temperature and $S_{30\ m}/T_{30\ m}$, seawater density data are given, and illustrate that this parameter does not show a better fit than the $S_{30\ m}/T_{30\ m}$ ratio. The regression between this averaged data from each region is ($S_{30\ m}/T_{30\ m}$)=(0.085*average process length+0.468), R^2=0.89 (Fig. 6).

3.3.1. Process length in relation to body diameter

No relation between the process length and cyst body diameter was found (R^2=0.002). This was expected since culture experiments also revealed no relation between the body diameter and the salinity (Hallet, 1999). Furthermore, no significant relation was found between body diameter with the ratio between salinity and temperature at different depths. Variations in cyst body diameter are probably caused mainly by germination of the cyst or compression.

3.3.2. Process length in relation to relative cyst abundance

Mudie et al. (2001) found a correlation of R^2=0.71 between the relative abundance of *L. machaerophorum* and increasing salinity between 16 and 21.5 psu for Holocene assemblages in Marmara Sea core M9. To check this relationship in our dataset, the relative abundances of *L. machaerophorum* were determined in 92 surface samples. No significant linear relation between relative abundances in the assemblages and either the process length or the body diameter was found. No significant relationship between relative abundance and temperature or salinity data was found. This is not surprising since the relationship between relative abundances and environmental parameters is not linear, but unimodal (Dale, 1996), and several other factors play a role in determining the relative abundances on such a global scale, mostly relative abundances of other species (closed-sum problems).

3.4. Confocal laser microscopy

All processes on 20 cysts from the North Adriatic Sea (samples AN71 and AN6b) and one from the Gulf of Cadiz (sample GeoB9064) were measured, resulting in 1460 process measurements. The average distances between the processes were also calculated. A summary of the results is given in Table 2. Process length ranged from 0 to 31 µm, which differs from the 1983 process lengths from the North Adriatic Sea samples measured with transmitted light microscopy (6 to 34 µm). The shift in the frequency size spectra was obviously due to the fact that only the longest processes were measured (Fig. 7). Most

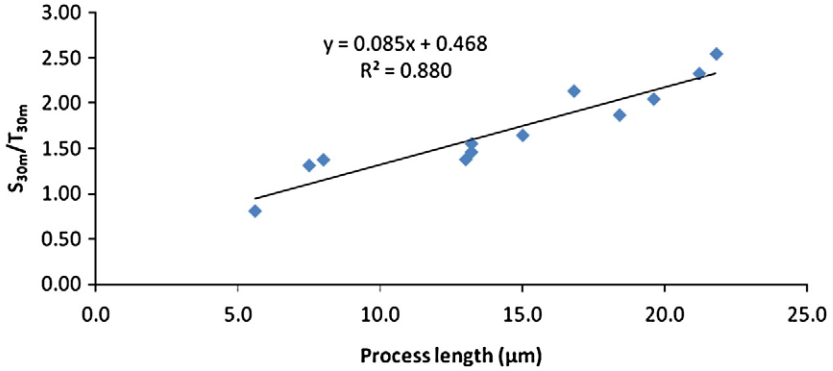

Fig. 6. Regression between average process length and summer $S_{30\ m}/T_{30\ m}$ averaged for every region separately.

Table 2
Average process length, standard deviation, number of processes measured and average distance between process bases from confocal microscopy in full measurements

Cyst number	Sample	Average length (µm)	Stdev length (µm)	# Processes measured	Body diameter (µm)	Average distance (µm)
2	AN71	9.82	5.78	79	44.53	4.35
4	AN71	7.26	5.72	89	39.84	3.76
5	AN71	15.87	5.06	50	56.89	5.79
7	AN71	9.80	6.36	72	45.11	4.68
9	AN71	17.79	6.41	62	43.25	6.78
10	AN71	10.32	6.49	67	39.95	4.55
11	AN71	12.25	1.90	56	43.26	6.21
12	AN71	6.85	4.82	107	39.34	3.98
13	AN71	11.50	7.26	89	43.32	4.76
14	AN71	15.88	7.27	61	51.76	6.90
15	AN71	13.20	6.19	28*	40.54	5.67
16	AN71	15.43	4.19	59	41.93	5.61
17	AN71	12.44	5.43	71	44.69	4.95
2	AN6B	11.79	6.09	71	36.38	4.40
4	AN6B	9.86	5.47	103	45.60	4.88
5	AN6B	9.14	7.13	102	42.87	4.05
6	AN6B	12.17	4.72	76	47.13	4.71
8	AN6B	12.53	4.53	58	57.84	5.66
9	AN6B	13.07	3.50	51	40.77	5.40
10	AN6B	10.30	4.68	76	41.20	4.44
1	GeoB9064	18.16	6.76	33	36.10	6.24
Average		12.16	5.51	69.52	43.92	5.13
Stdev		3.11	1.33	21.06	5.68	0.91

*This number was not used in the regression with process length, since less than half of this cyst was preserved.

remarkable was the large peak around 3 µm for the confocal measurements. Apparently, a large number of shorter processes were present on most of these cysts.

It is noteworthy that the number of processes was significantly inversely related to the average process length (R^2=0.65) (Fig. 8) and the average process length was significantly related to the average distance between the processes (R^2=0.78) (Fig. 9), and that. The lower R^2 can be explained by the incompleteness of the cysts: all cysts were germinated and thus lacking opercular plates, which can number between one and five or more in the case of epicystal archeopyles (Evitt, 1985). This implies that a large number of processes can be missing, and it would be subjective to attempt a correction for the missing processes. It was not possible to use encysted specimens since the strong autofluorescence of the endospore of these specimens obscured many of the least autofluorescent processes. No significant relation was found between the body diameter and the average process length (R^2=0.04), which supports the observation with transmitted light microscopy.

4. Discussion

4.1. Process length correlated to summer $S_{30\ m}/T_{30\ m}$: is it realistic?

The quasi unimodal size frequency spectrum of both process length and cyst body diameter (Figs. 2 and 3), plus the correlation between the average process length and the summer $S_{30\ m}/T_{30\ m}$, strongly confirm that all recorded cysts are ecophenotypes of a single species. It is furthermore not surprising that the most significant relation was found with the summer $S_{30\ m}/T_{30\ m}$ depth. These three extra parameters – seasonality, temperature and depth – are discussed below.

Late summer–early autumn is generally the time of maximum stratification of the surface waters. Reduced salinity would enhance the water column stability with the generation of a pycnocline, and lowered water column turbulence, conditions that favour growth of *L. polyedrum* (Thomas and Gibson, 1990). In most upwelling regions, this would coincide with periods of upwelling relaxation (Blasco, 1977). Late summer–early autumn is the time of the exponential growth phase of *L. polyedrum*, which coincides with peak production of *L. machaerophorum* cysts, at least in Loch Creran, northwest Scotland (Lewis et al., 1985), and in Todos Santos Bay, Mexico (Peña-Manjarrez et al., 2005). Culturing suggests that the cyst production is triggered by nutrient depletion, and influenced by temperature (Lewis and Hallett, 1997).

The relationship found between process length and both temperature and salinity is not surprising since the formation of processes can be considered a biochemical process (Hallett, 1999), dependent on both temperature (negative relation) and salinity (positive relation). The culture experiments by Hallett (1999) confirm a positive relation to salinity and a negative relation to temperature.

Moreover, the cysts are probably formed deeper in the water column, which would explain the fit to a 30 m depth. It is well known that *L. polyedrum* migrates deep in the water column (Lewis and Hallett, 1997). A similar vertically migrating dinoflagellate, *Peridiniella catenata,* also forms cysts deeper in the water column, mostly at 30–40 m depth (Spilling et al., 2006). These cysts are probably formed within a range of water depths, and with 30 m depth reflecting an average depth.

The ranges of temperature (9–31 °C) and salinity (12.4–42.1 psu) at 30 m represent the window in which cyst formation takes place. Cultures show that *L. polyedrum* forms cysts at salinities ranging from 10 to 40 psu (Hallett, 1999), which fits with the results obtained in this study. The relation to deeper salinity and temperature data suggests that cyst formation more often than not takes place deeper in the water column, where salinities may be higher and temperatures lower, which suggests that caution is needed before linking *L. machaerophorum* cyst abundances directly to near surface data. This

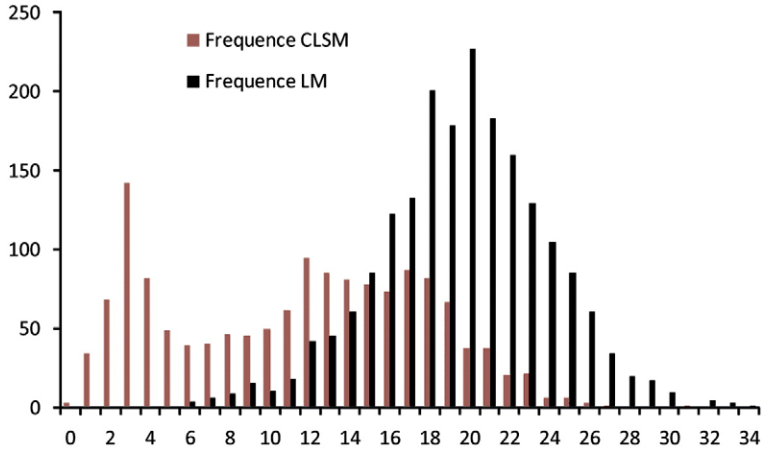

Fig. 7. Comparison between the size-frequency spectra from 1460 confocal measurements (CLSM) from the North Adriatic Sea (samples AN71 and AN6b) and from the Gulf of Cadiz and 1983 light microscope (LM) measurements from the North Adriatic.

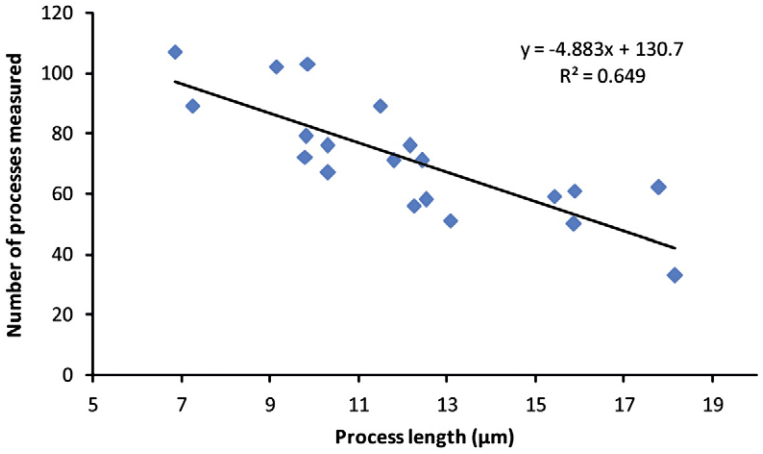

Fig. 8. Regression between average process length and the number of processes for the cysts measured with confocal microscopy.

could explain the occurrence of cysts of *L. polyedrum* in regions with surface salinities as low as 5 psu (e.g. McMinn, 1990, 1991; Dale, 1996; Persson et al., 2000).

No better relation was found with density despite its dependence on salinity and temperature. Apparently, density as calculated from salinity and temperature, and pressure (water depth) by Fofonoff and Millard (1983) is much more determined by salinity, and less by temperature, whereas we assume that measured average process length is influenced by a combination of these parameters.

4.2. Transport issues

L. polyedrum occurs in estuaries, coastal embayments and neritic environments of temperate to subtropical regions (Lewis and Hallett, 1997). However, transport of the cysts into other areas by currents must be considered, and the records of *L. machaerophorum* in oceanic environments have been attributed to reworking or long-distance transport (Wall et al., 1977). A classic example is the upwelling area off northwest Africa where the cyst has been recorded over a much wider area than the thecate stage (Dodge and Harland, 1991). In this study, it was assumed that long-distance transport was not an important factor, since the transported cysts would be transported from areas with minor salinity and temperature differences, which would, according to the equation (see 2.3), be reflected in negligible changes in process length.

4.3. The Problematic Kattegat–Skagerrak and Scandinavian Fjord samples

It is noteworthy that the inclusion of the Kattegat–Skagerrak and Scandinavian samples increased the scatter of the regression significantly. Two causes can be suggested. Firstly, since most samples plotted above the regression line, the average process length could be anomalously short. Most probably this is not linked to a preservation issue, since the average preservation was average to good (except for the Risör site), and broken processes were rare. All recovered cysts are from the uppermost section of box cores, and are thus recently formed. One possible explanation is that these specimens are genetically different which could result in slightly different morphologies. However, there is no *a priori* reason why this should be so, and this conflicts with the unimodal size-frequency distribution of process length.

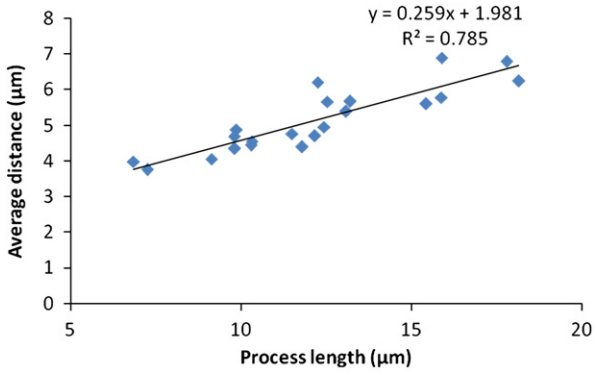

Fig. 9. Regression between average process length and the average distance between process bases for the cysts measured with confocal microscopy.

Secondly, the used summer $S_{30\ m}/T_{30\ m}$ data could be incorrect, and this can be attributed to several causes. On one hand, the cyst production could have taken place at different water depths. When surface data ($S_{0\ m}/T_{0\ m}$) for the Kattegat–Skagerrak and Scandinavian samples is included in the global dataset of summer $S_{30\ m}/T_{30\ m}$, the relation between average process length is more significant ($R^2 = 0.61$). On the other hand, the timing of cyst production might be different. *L. polyedrum* blooms in fjords are probably short-lived, followed by a long resting period (Godhe and McQuoid, 2003). As for the Kattegat–Skagerrak, salinity-driven stratification, with higher salinity bottom waters and low salinity surface waters, could result in a very particular environment. In this way, the cysts are formed probably under specific salinity and temperature conditions, which could explain the increase in scatter.

4.4. Confocal measurements and implications for cyst formation

The results of this study lead to enhanced insight into the process of cyst formation of *L. machaerophorum*. Before discussing the implications of our study in detail we summarise the state of the art knowledge on cyst formation as described by Lewis & Hallett (1997) and Kokinos and Anderson (1995). The studies of these authors indicate that at the start of the cyst formation process, the motile planozygote ceases swimming, ejects its flagella, and the outer membrane swells. Then, the thecal plates of the planozygote dissociate and are pulled away from the cytoplasm by the ballooning of the outer membrane and underneath this, the formation of the cyst wall occurs. A layer of globules (each ~5 µm across) surround the cytoplasm and the spines grow outwards taking the globules with them. These terminal globules collapse to form spine tips and variations in this process confer the variable process morphology observed. Probably, membrane expansion is activated by osmosis (Kokinos, 1994), which causes a pressure gradient. According to Hallett (1999) the outer membrane always reaches full expansion, both for short and long process-bearing individuals. Measurements with confocal laser microscopy clearly show that a positive relation exists between the process length and the distance between processes, and a negative relation between the processes length and the number of processes.

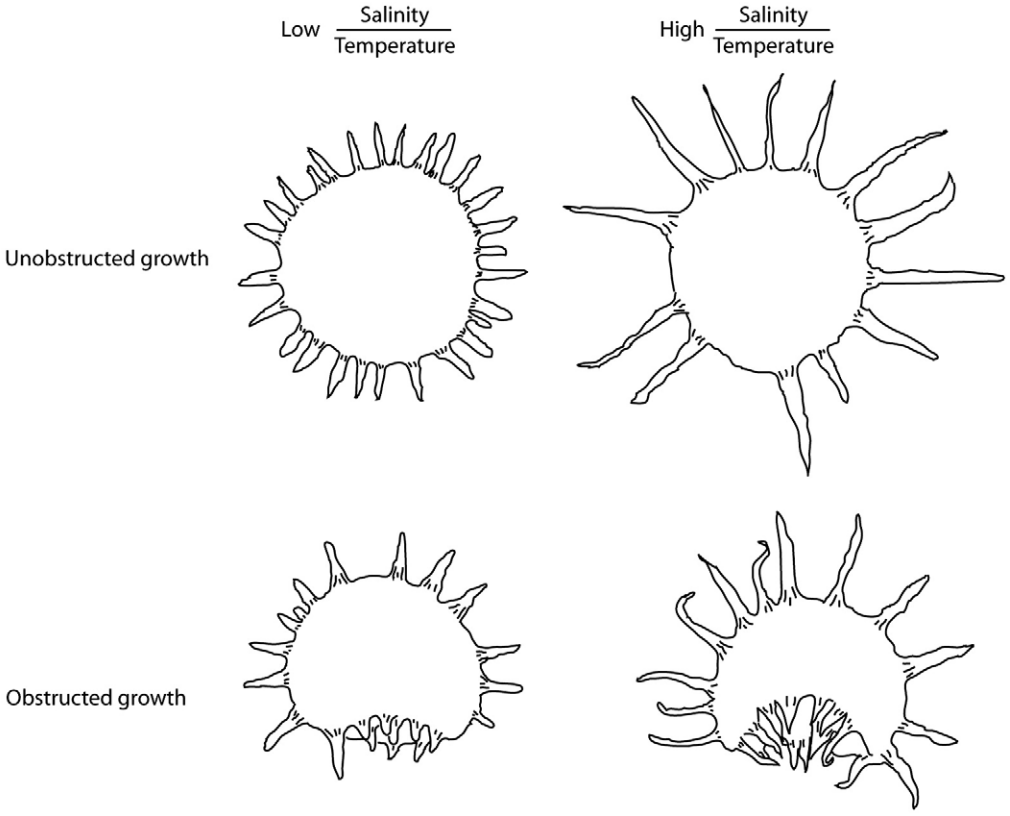

Fig. 10. Conceptual model for process formation.

These findings lead towards three implications. Firstly, the amount of dinosporin necessary for constructing the processes would be constant, at least for the studied cysts from the Mediterranean Sea. However, one needs to assume that the amount of dinosporin is proportionate to the number of processes, multiplied by the average process length. This entails that that the amount of dinosporin needed for formation of the periphragm is constant, which is reasonable since the body diameter is independent of process length. Secondly, the good correlation between the average distance and the process length, together with the observation that globules are all forming simultaneously (Hallett, pers. comm.), suggests that the process length is predetermined. Thirdly, these observations suggest the existence of two end members: one with many closely spaced short processes, and one with a few, more widely spaced, long processes (Fig. 10). This gradient in biometrical groups can also be visually observed in transmitted light microscopy (Plate I–IV) and the suggested formation process for the two end members is illustrated in Fig. 11.

In order to reconcile these observations with observations from cultures, the physico-chemical properties of dinosporin have to be considered. According to Kokinos (1994), dinosporin consists of a complex aromatic biopolymer, possibly made of tocopherols. However, upon reanalysis, De Leeuw et al. (2006) showed the tocopherol link to be untrue. It can now be speculated that a certain fixed amount of this precursor monomer (probably a sugar, Versteegh, pers. comm.) for dinosporin is distributed across the sphere, in such a way that a minimum of energy is necessary for this process. This can occur through a process of flocculation (Hemsley et al. (2004)), and is dependent on both temperature and salinity. Fewer but larger colloids of the monomer will be formed when $S_{30\ m}/T_{30\ m}$ is higher and these will coalesce on the cytoplasmic membrane. When many small colloids are formed, it might occur that two or more colloids merge, and form one larger process (Plates II.13, II.15 and II.22). This theory can also explain the rare occurrence of crests on cyst species such as *Operculodinium centrocarpum*, where crests are

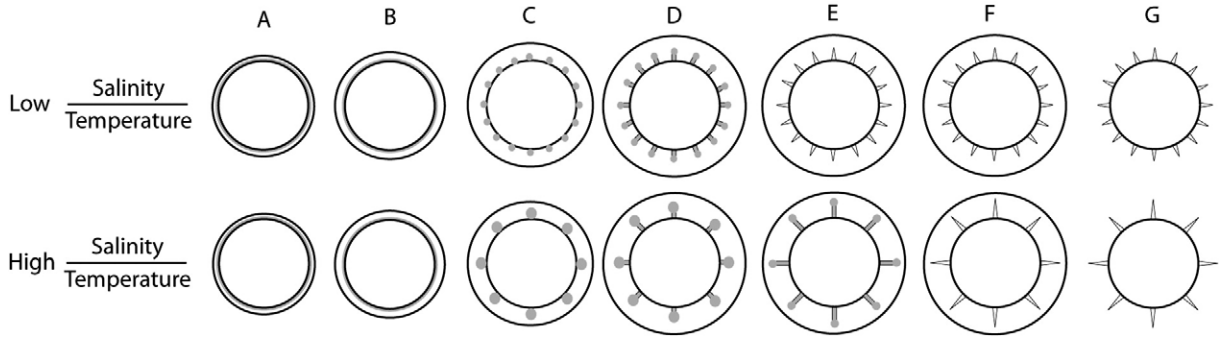

Fig. 11. Suggested formation process for the two end members based on observation and documentation by Kokinos and Anderson (1995) and Hallett (1999), and theoretical consideration by Hemsley et al. (2004). Monomer is shown in grey, membranes and polymerised coat in black. (A–B) The outer membrane starts to expand, a fixed amount of monomer is formed and starts to coalesce on the cytoplasmic membrane. (C) Depending on environmental parameters (salinity and temperature), a lot of small or a few large colloids of the monomer are formed. (D) Visco-elastic dinosporin is synthesized on the globules and stretches in a radial direction. (E) Membrane expansion often comes to a stop before radial stretching ends. (F) Formation of longer process takes longer than shorter process formation. (G) Membrane rupture occurs.

formed when processes are closely spaced. In the next step, the viscoelastic dinosporin is synthesized on the globules, and stretches out in a radial direction. This stretching is clearly visible in the striations at the base of the processes. Another result of this stretching is the formation of tiny spinules at the distal tip. These are more apparent on the longer processes, and could be the result of a fractal process: what happens at a larger scale, namely the stretching of the processes, is repeated here at a smaller scale as, stretching of the spinules. However, it is unlikely that the stretching is solely caused by membrane expansion. Hallett (1999) indicated that the outer membrane expansion is independent of the definitive process length. Thus the stretching is most probably caused by the combination of outer membrane expansion and a chemical process, similar to the swelling of cysts caused by acetolysis or KOH (see Section 2.1).

Two types of cysts deserve special attention. Clavate or bulbous process bearing cysts (Plate I.6; Plate II.11, II.20) were frequently encountered in surface sediments from low salinity environments (Black Sea, Caspian Sea, Aral Sea and the Kattegat–Skagerrak). They were frequently encountered in culture by Kokinos and Anderson (1995), but rarely by Hallett (1999). These only seem to differ from normal processes, in that the globules were not able to detach from these processes. This is supported by the fact that the length of normal processes on cysts bearing clavate processes is the same as for clavate processes.

The second type of cysts deserving attention are the bald or spheromorphic cyst. Lewis and Hallett (1997) observed that these cysts are not artefacts of laboratory culturing, since cysts devoid of processes occur in the natural environment of Loch Creran in northwest Scotland. Moreover, Persson (unpubl. experiment, 1996) noted inculturing experiments, that these cysts are viable, and thus cannot be regarded as malformations. Apart from the Aral Sea, very few bald cysts were recorded in surface sediments. It appears that on these cysts, process development did not take place. It can be speculated that this could be caused by a very early rupture of the outer membrane or the inability of the precursor monomer to flocculate at a very reduced $S_{30\ m}/T_{30\ m}$.

4.5. Process distribution

The process distribution on *L. machaerophorum* has been considered intratabular to non-tabular (Wall and Dale, 1968), although some authors noted alignment in the cingular area (Evitt and Davidson, 1964, Wall et al., 1973). Marret et al. (2004) showed a remarkable reticulate pattern in the ventral area on cysts with very short processes from the Caspian Sea, suggestive of a tabular distribution. Our findings indicate a regular and equidistant distribution of the processes, with evidence of a tabulation pattern lacking.

The process length distribution is not uniform. In cultures, cysts are formed at the bottom of the observation chambers, resulting in an asymmetrical distribution of the processes on the cysts, where shorter processes are formed at the obstructed side, and longer processes at the unobstructed side (Kokinos and Anderson, 1995; Hallett, 1999). When assuming that a constant amount of dinosporin is distributed over the cyst body, aberrantly long processes would form at the unobstructed side, and aberrantly short processes at the obstructed side. Our observations confirm this phenomenon: cysts from shallow areas show a similar asymmetry. The frequent occurrence of short processes on cysts from shallow areas in the Mediterranean Sea can be explained in a similar way (Fig. 7). If one measures the longest processes on these cysts, values will be slightly larger than expected from our equation. This obstruction factor needs to be incorporated into our conceptual model (Fig. 10). It is furthermore noticeable that many of the non-shallow cysts show this asymmetry to a certain degree (Plate I–IV), suggesting that this obstruction could be occurring more generally. The frequent occurrence of short processes along the cingulum could also be explained in a similar way, if the cysts were to be formed in a preferred orientation, with the obstructed side along the archeopyle.

4.6. Biological function of morphological changes?

The final consideration deals with the biological function of the processes. Possible functions of spines on resting stages have been proposed by Belmonte et al. (1997), and include flotation, clustering and enhanced sinking, passive defence, sensory activity and/or chemical exchanges and dispersal. Since the link between process length and $S_{30\ m}/T_{30\ m}$ exists and density is also dependent on $S_{30\ m}/T_{30\ m}$, it is obvious that either flotation or clustering and enhanced sinking will be the most important biological function of morphological changes of the processes. Longer processes increase the drag coefficient of the cyst and thus increase floating ability according to Stokes' law, but also increase cluster ability. However, the longest processes occur in high water density (high $S_{30\ m}/T_{30\ m}$) environments, where floatation would be easier, which is counterintuitive. It seems more logical, then, that longer processes are developed to facilitate sinking (through clustering) in environments with high water density.

5. Conclusions

- A total of 19,611 measurements of *L. machaerophorum* from 144 globally distributed surface samples showed a relationship between process length and both summer salinity and temperature at 30 m water depth, as given by the following equation: $(S_{30\ m}/T_{30\ m}) = (0.078 * \text{average process length} + 0.534)$ with $R^2 = 0.69$. For salinity the range covered is at least 12.5 to 42 psu, and for temperature 9 to 31 °C. To establish the accuracy of this salinity proxy, future culture studies will hopefully further constrain this relationship.
- Confocal microscopy shows that distances between processes are strongly related to average process length, and that the number of processes is inversely related to average process length. This suggests a two end-member model, one with numerous short, closely spaced processes and one with relatively few, widely spaced, long processes.
- Processes of *L. machaerophorum* are hypothesized to biologically function mainly as a clustering device to enhance sinking rates.

Acknowledgements

Warner Brückmann and Silke Schenk (IFM Geomar), Rusty Lotti Bond (Lamont Doherty Earth Observatory), Chad Broyles and Walter Hale (IODP), Jim Broda Braddock Linsley (University at Albany-State), Larry Benson (USGS), Aurélie Chambouvet and Nathalie Simon (Station Biologique, Roscoff) and Liviu Giosan (WHOI), Gilles Lericolais (IFREMER, France), Katrien Heirman and Hans Pirlet (RCMG), Jean-Pierre Arrondeau (IAV) and Rex Harland are kindly acknowledged for providing samples.

Marie-Thérèse Morzadec-Kerfourn is kindly thanked for providing detailed information on sampling locations from Brittany and Philippe Picon (GIPREB) for providing salinity data from Etang de Berre. We are grateful to Zoë Verlaak for helping out with the confocal measurements and Richard Hallett for stimulating discussions on *Lingulodinium machaerophorum* process development.

We express gratitude to Martin Head and one anonymous reviewer for detailed reviews of an earlier version of this manuscript.

Appendix A. Supplementary data

Supplementary data associated with this article can be found, in the online version, at doi:10.1016/j.marmicro.2008.10.004.

References

Amo rim, A., Palma, A.S., Sampayo, M.A., Moita, M.T., 2001. On a *Lingulodinium polyedrum* bloom in Setúbal bay, Portugal. In: Hallegraeff, G.M., Blackburn, S.I., Bolch, C.J., Lewis, R.J. (Eds.), Harmful Algal Blooms 2000. Intergovernmental Oceanographic Commission of UNESCO, pp. 133–136.

Bendle, J., Rosell-Mele, A., Ziveri, P., 2005. Variability of unusual distributions of alkenones in the surface waters of the Nordic seas. Paleoceanography 20. doi:10.1029/2004PA001025.

Bennouna, A., Berland, B., El Attar, J., Assobhei, O., 2002. *Lingulodinium polyedrum* (Stein) Dodge red tide in shellfish areas along Doukkala coast (Moroccan Atlantic). Oceanologica Acta 25 (3), 159–170.

Belmonte, G., Miglietta, A., Rubino, F., Boero, F., 1997. Morphological convergence of resting stages of planktonic organisms: a review. Hydrobiologia 355, 159–165.

Blasco, D., 1977. Red tide in the upwelling region of Baja California. Limnology and Oceanography 22, 255–263.

Bollmann, J., Herrle, J.O., 2007. Morphological variation of *Emiliania huxleyi* and sea surface salinity. Earth and Planetary Science Letters 255, 273–288.

Boyer, T.P., Stephens, C., Antonov, J.I., Conkright, M.E., Locarnini, R.A., O'Brien, T.D., Garcia, H.E., 2002. World Ocean Atlas 2001, Volume 2: salinity. In: Levitus, S. (Ed.), NOAA Atlas NESDIS, vol. 50. U.S. Government Printing Office, Wash., D.C. 165 pp., CD-ROMs.

Brenner, W., 2005. Holocene environmental history of the Gotland Basin (Baltic Sea) — a micropalaeontological model. Palaeogeography, Palaeoclimatology, Palaeoecology 220, 227–241.

Cagatay, M.N., Görür, N., Algan, O., Eastoe, C., Tchapalyga, A., Ongan, D., Kuhn, T., Kuscu, I., 2000. Late Glacial–Holocene palaeoceanography of the Sea of Marmara: timing of connections with the Mediterranean and the Black Seas. Marine Geology 167, 191–206.

Caner, H., Algan, O., 2002. Palynology of sapropelic layers from the Marmara Sea. Marine Geology 190, 35–46.

Christensen, J.T., Cedhagen, T., Hylleberg, J., 2004. Late-Holocene salinity changes in Limfjorden, Denmark. Sarsia 89, 379–387.

Combourieu-Nebout, N., Londeix, L., Baudin, F., Turon, J.-L., von Grafenstein, R., Zahn, R., 1999. Quaternary marine and continental paleoenvironments in the western Mediterranean (site 976, Alboran Sea): Palynological evidence. Proceedings of the Ocean Drilling Program. Scientific Results, 161, pp. 457–468.

Dale, B., 1996. Dinoflagellate cyst ecology: modelling and geological applications. In: Jansonius, J., McGregor, D.C. (Eds.), Palynology: Principles and Applications, vol. 3. AASP Foundation, Dallas, TX, pp. 1249–1275.

Deflandre, G., Cookson, I.C., 1955. Fossil microplankton from Australia late Mesozoic and Tertiary sediments. Australian journal of Marine and Freshwater Research 6, 242–313.

de Leeuw, J.W., Versteegh, G.J.M., van Bergen, P.F., 2006. Biomacromolecules of algae and plants and their fossil analogues. Plant Ecology 182, 209–233.

de Vernal, A., Hillaire-Marcel, C., 2000. Sea-ice cover, sea-surface salinity and halo/thermocline structure of the northwest North Atlantic: modern versus full glacial conditions. Quaternary Science Reviews, 19 (5), 65–85.

Dodge, J.D., Harland, R., 1991. The distribution of planktonic dinoflagellates and their cysts in the eastern and northeastern Atlantic Ocean. New Phytologist 118, 593–603.

Ellegaard, 2000. Variations in dinoflagellate cyst morphology under conditions of changing salinity during the last 2000 years in the Limfjord, Denmark. Review of Palaeobotany and Palynology 109, 65–81.

Evitt, W.R., Davidson, S.E., 1964. Dinoflagellate cysts and thecae. Stanford University Publications Geological Sciences 10, 1–12.

Evitt, W.R., 1985. Sporpollenin dinoflagellate cysts. Their morphology and interpretation. Dallas: American Association of Stratigraphic Palynologists Foundation.

Fofonoff, P., Millard Jr., R.C., 1983. Algorithms for computing of fundamental properties of seawater. Unesco Technical Papers in Marine Sciences 44, 1–53.

Godhe, A., McQuoid, 2003. Influence of benthic and pelagic environmental factors on the distribution of dinoflagellate cysts in surface sediments along the Swedish west coast. Aquatic Microbial Ecology 32, 185–201.

Grøsfjeld, K., Harland, R., 2001. Distribution of modern dinoflagellate cysts from inshore areas along the coast of southern Norway. Journal of Quaternary Science 16 (7), 651–659.

Gundersen, N., 1988. En palynologisk undersøkelse av dinoflagellatcyster langs en synkende salinitetsgradient I recente sedimenter fra Østersjø-området. Unpublished candidata scientiarum thesis, University of Oslo, 1-96.

Hallett, R.I. 1999. Consequences of environmental change on the growth and morphology of *Lingulodinium polyedrum* (Dinophyceae) in culture. PhD thesis 1–109. University of Westminster.

Head, M.J., 1996. Late Cenozoic dinoflagellates from the Royal Society borehole at Ludham, Norfolk, Eastern England. Journal of Paleontology 70 (4), 543–570.

Hemsley, A.R., Lewis, J., Griffiths, P.C., 2004. Soft and sticky development: some underlying reasons for microarchitectural pattern convergence. Review of Palaeobotany and Palynology 130, 105–119.

Kokinos, J.P., 1994. Studies on the cell wall of dinoflagellate resting cysts: morphological development, ultrastructure, and chemical composition. PhD thesis, Massachusetts Institute of Technology/Woods Hole Oceanographic Institution.

Kokinos, J.P., Anderson, D.M., 1995. Morphological development of resting cysts in cultures of the marine dinoflagellate *Lingulodinium polyedrum* (= *L. machaerophorum*). Palynology 19, 143–166.

Kotthoff, U., Pross, J., Müller, U.C., Peyron, O., Schmiedl, G., Schulz, H., Bordon, A., 2008. Climate dynamics in the borderlands of the Aegean Sea during formation of sapropel S1 deduced from a marine pollen record. Quaternary Science Reviews 27, 832–845.

Kuhlmann, H., Freudenthal, T., Helmke, P., Meggers, H., 2004. Reconstruction of paleoceanography off NW Africa during the last 40,000 years: influence of local and regional factors on sediment accumulation. Marine Geology 207 (1–4), 209–224.

Leroy, S.A.G., Marret, F., Giralt, S., Bulatov, S.A., 2006. Natural and anthropogenic rapid changes in the Kara-Bogaz Gol over the last two centuries reconstructed from palynological analyses and a comparison to instrumental records. Quaternary International 150, 52–70.

Leroy, S.A.G., Marret, F., Gibert, E., Chalie, F., Reyss, J.L., Arpe, K., 2007. River inflow and salinity changes in the Caspian Sea during the last 5500 years. Quaternary Science Reviews 26 (25–28), 3359–3383.

Leroy, V., 2001. Traceurs palynologiques des flux biogéniques et des conditions hydrographiques en milieu marin cotier: exemple de l'étang de Berre. DEA, Ecole doctorale Sciences de l'environment d'Aix-Marseille, 30 pp.

Lewis, J., Tett, P., Dodge, J.D., 1985. The cyst-theca cycle of *Gonyaulax polyedra* (*Lingulodinium machaerophorum*) in Creran, a Scottish west coast Sea-Loch. In: Anderson, D.M., White, A.W., Baden, D.G. (Eds.), Toxic dinoflagellates. Elsevier Science Publishing, pp. 85–90.

Lewis, J., Hallett, R., 1997. *Lingulodinium polyedrum* (*Gonyaulax polyedra*) a blooming dinoflagellate. In: Ansell, A.D., Gibson, R.N., Barnes, M. (Eds.), Oceanography and Marine Biology: An Annual Review, vol. 35. UCL Press, London, pp. 97–161.

Marret, F., 1994. Distribution of dinoflagellate cysts in recent marine sediments from the east Equatorial Atlantic (Gulf of Guinea). Review of Palaeobotany and Palynology 84, 1–22.

Marret, F., Scource, J., 2002. Control of modern dinoflagellate cyst distribution in the Irish and Celtic seas by seasonal stratification dynamics. Marine Micropaleontology 47, 101–116.

Marret, F., Leroy, S.A.G., Chalié, F., Gasse, F., 2004. New organic-walled dinoflagellate cysts from recent sediments of Central Asian seas. Review of Palaeobotany and Palynology 129, 1–20.

Marret, F., Zonneveld, K.A.F., 2003. Atlas of modern organic-walled dinoflagellate cyst distribution. Review of Palaeobotany and Palynology 125, 1–200.

Marret, F., Mudie, P., Aksu, A., Hiscott, R.N., 2007. A Holocene dinocyst record of a two-step transformation of the Neoeuxinian brackish water lake into the Black Sea. Quaternary International 193. doi:10.1016/j.quaint.2007.01.010.

Matthiessen, J., Brenner, W., 1996. Chlorococcalalgen und Dinoflagellaten-Zysten in rezenten Sedimenten des Greifswalder Boddens (südliche Ostsee). Senckenbergiana Maritima 27 (1/2), 33–48.

Mertens, K., Lynn, M., Aycard, M., Lin, H.-L., Louwye, S., 2008. Coccolithophores as paleoecological indicators for shift of the ITCZ in the Cariaco Basin during the Late Quaternary. Journal of Quaternary Science. doi:10.1002/jqs.1194.

McMinn, A., 1990. Recent dinoflagellate cyst distribution in eastern Australia. Review of Palaeobotany and Palynology 65, 305–310.

McMinn, A., 1991. Recent dinoflagellate cysts from estuarieson the central coast of New South Wales, Australia. Micropaleontology 37, 269–287.

Mudie, P.J., Aksu, A.E., Yasar, D., 2001. Late Quaternary dinoflagellate cysts from the Black, Marmara and Aegean seas: variations in assemblages, morphology and paleosalinity. Marine Micropaleontology 43, 155–178.

Mudie, P.J., Rochon, A.E., Levac, E., 2002. Palynological records of red tide-producing species in Canada: past trends and implications for the future. Palaeogeography, Palaeoclimatology, Palaeoecology 180 (1), 159–186.

Mudie, P.J., Marret, F., Aksu, A.E., Hiscott, R.N., Gillespie, H., 2007. Palynological evidence for climatic change, anthropogenic activity and outflow of Black Sea water during the Late Pleistocene and Holocene: centennial- to decadal-scale records from the Black and Marmara Seas. Quaternary International 167–168, 73–90.

Nehring, S., 1994. Spatial distribution of dinoflagellate resting cysts in recent sediments of Kiel Bight, Germany (Baltic Sea). Ophelia 39 (2), 137–158.

Nehring, S., 1997. Dinoflagellate resting cysts from recent German coastal sediments. Botanica Marina 40, 307–324.

Nürnberg, D., Groeneveld, J., 2006. Pleistocene variability of the subtropical convergence at East Tasman Plateau: evidence from planktonic foraminiferal Mg/Ca (ODP Site 1172A). Geochemistry, Geophysics, Geosystems 7–4, Q04P11. doi:10.1029/2005GC000984.

Peña-Manjarrez, J.L., Helenes, J., Gaxiola-Castro, G., Orellano-Cepeda, E., 2005. Dinoflagellate cysts and bloom events at Todos Santos Bay, Baja California, México, 1999–2000. Continental Shelf Research 25, 1375–1393.

Persson, A., Godhe, A., Karlson, B., 2000. Dinoflagellate cysts in recent sediments from the West coast of Sweden. Botanica Marina 43, 66–79.

Pospelova, V., de Vernal, A., Pedersen, T.F., 2008. Distribution of dinoflagellate cysts in surface sediments from the northeastern Pacific Ocean (43–25°N) in relation to sea-surface temperature, productivity and coastal upwelling. Marine Micropaleontology 68 (1–2), 21–48. doi:10.1016/j.marmicro.2008.01.008.

Reid, P.C., 1974. Gonyaulacean dinoflagellate cysts from the British Isles. Nova Hedwigia 25, 579–637.

Richter, D., Vink, A., Zonneveld, K.A.F., Kuhlmann, H., Willems, H., 2007. Calcareous dinoflagellate cyst distributions in surface sediments from upwelling areas off NW Africa, and their relationships with environmental parameters of the upper water column. Marine Micropaleontology 63, 201–228.

Robert, C., Degiovanni, C., Jaubert, R., Leroy, V., Reyss, J.L., Saliège, J.F., Thouveny, N., de Vernal, A., 2006. Variability of sedimentation and environment in the Berre coastal lagoon (SE France) since the first millennium: natural and anthropogenic forcings. Journal of Geochemical Exploration 88, 440–444.

Rostek, F., Ruhland, G., Bassinot, F.C., Muller, P.J., Labeyrie, L.D., Lancelot, Y., Bard, E., 1993. Reconstructing sea-surface temperature and salinity using $\delta^{18}O$ and alkenone records. Nature 364, 319–321.

Sangiorgi, F., Fabbri, D., Comandini, M., Gabbianelli, G., Tagliavini, E., 2005. The distribution of sterols and organic-walled dinoflagellate cysts in surface sediments of the Northwestern Adriatic Sea (Italy). Estuarine, Coastal and Shelf Science 64, 395–406.

Schmidt, M.W., Spero, H.J., Lea, D.W., 2004. Links between salinity variation in the Caribbean and North Atlantic thermohaline circulation. Nature 428, 160–163.

Schoell, M., 1974. Valdivia VA 01/03, Hydrographie II und III. Bundesanstalt für Bodenforschung, Hannover, Germany.

Schouten, S., Ossebaar, J., Schreiber, K., Kienhuis, M.V.M., Langer, G., Benthien, A., Bijma, J., 2006. The effect of temperature, salinity and growth rate on the stable hydrogen isotopic composition of long chain alkenones produced by *Emiliania huxleyi* and *Gephyrocapsa oceanic*. Biogeosciences 3, 113–119.

Sorrell, P., Popescu, S.-M., Head, M.J., Suc, J.-P., Klotz, S., Oberhänsli, H., 2006. Hydrographic development of the Aral Sea during the last 2000 years based on a quantitative analysis of dinoflagellate cysts. Palaeography, Palaeoclimatology, Palaeoecology 234, 304–327.

Spilling, K., Kremp, A., Tamelander, T., 2006. Vertical distribution and cyst production of *Peridiniella catenata* (Dinophyceae) during a spring bloom in the Baltic Sea. Journal of Plankton Research 28 (7), 659–665.

Stephens, C., Antonov, J.I., Boyer, T.P., Conkright, M.E., Locarnini, R.A., O'Brien, T.D., Garcia, H.E., 2002. World Ocean Atlas 2001, Volume 1: temperature. In: Levitus, S. (Ed.), NOAA Atlas NESDIS, vol. 49. U.S. Government Printing Office, Wash., D.C. 167 pp., CD-ROMs.

Sweeney, B.M., 1975. Red tides I have known. In *toxic dinoflagellate blooms*. In: LoCicero, V.R. (Ed.), Massachusetts Science and Technology Foundation, Wakefield, Massachusetts, pp. 225–234.

Thomas, W.H., Gibson, C.H., 1990. Quantified small-scale turbulence inhibits a red tide dinoflagellate, *Gonyaulax polyedra* Stein. Deep-Sea Research 37, 1538–1593.

Turon, J.-L., 1984. Le palynoplankton dans l'environment actuel de l'Atlantic nord-oriental. Evolution climatique et hydrologique depuis le dernier maximum glaciaire. Mémoire de l'institut de Géologie du Bassin d'Aquitaine 17, 1–313.

van der Meer, M.T.J., Sangiorgi, F., Baas, M., Brinkhuis, H., Sinninghe-Damsté, J.S., Schouten, S., 2008. Molecular isotopic and dinoflagellate evidence for Late Holocene freshening of the Black Sea. Earth and Planetary Science Letters 267, 426–434.

Van der Meer, M.T.J., Baas, M., Rijpstra, W.I.C., Marino, G., Rohling, E.J., Sinninghe Damsté, J.S., Schouten, S., 2007. Hydrogen isotopic compositions of long-chain alkenones record freshwater flooding of the Eastern Mediterranean at the onset of sapropel deposition. Earth and Planetary Science Letters 262, 594–600.

van Harten, D., 2000. Variable noding in *Cyprideis torosa* (Ostracoda, Crustacea): an overview, experimental results and a model from Catastrophe Theory. Hydrobiologia 419 (1), 131–139. doi:10.1023/A:1003935419364.

Verleye, T., Mertens, K.N., Louwye, S., Arz, H.W., 2008. Holocene Salinity changes in the southwestern Black Sea: a reconstruction based on dinoflagellate cysts. Palynology 32.

Vink, A., Rühlemann, C., Zonneveld, K.A.F., Mulitza, S., Hüls, M., Willems, H., 2001. Shifts in the position of the North Equatorial Current and rapid productivity changes in the western Tropical Atlantic during the last glacial. Paleoceanography 16 (1), 1–12.

Vink, A., Zonneveld, K.A.F., Willems, H., 2000. Organic-walled dinoflagellate cysts in western equatorial Atlantic surface sediments: distributions and their relation to environment. Review of Palaeobotany and Palynology 112, 247–286.

Wall, D., Dale, B., 1968. Modern dinoflagellate cysts and the evolution of the Peridiniales. Micropaleontology 14, 265–304.

Wall, D., Dale, B., Harada, K., 1973. Description of new fossil dinoflagellates from the Late Quaternary of the Black Sea. Micropaleontology 19, 18–31.

Wall, D., Dale, B., Lohman, G.P., Smith, W.K., 1977. The environmental and climatic distribution of dinoflagellate cysts in modern marine sediments from regions in the North and South Atlantic Ocean and adjacent seas. Marine Micropaleontology 2, 121–200.

Wang, L., Sarntheim, M., Duplessy, J.C., Erlenkeuser, H., Jung, S., Pfaumann, U., 1995. Paleo sea surface salinities in the low-latitude Atlantic: the $\delta^{18}O$ record of *Globigerinoides ruber* (White). Paleoceanography 10, 749–761.

Zonneveld, K.A.F., Versteegh, G.J.M., de Lange, G.J., 2001. Palaeoproductivity and post-depositional aerobic organic matter decay reflected by dinofagellate cyst assemblages of the Eastern Mediterranean S1 sapropel. Marine Geology 172, 181–195.